arXiv:cond-mat/0406308v1 [cond-mat.mtrl-sci] 14 Jun 2004

Microscopic Calculation of Flow Stress in Cu-Mg Metallic Glass

Nicholas P. Bailey,[1,*] Jakob Schiøtz,[2] and Karsten W. Jacobsen[2]

[1] *CAMP, Department of Physics, Technical University of Denmark, 2800 Lyngby, Denmark and Materials Research Department, Risø National Laboratory, DK-4000, Roskilde, Denmark*

[2] *CAMP, Department of Physics, Technical University of Denmark, 2800 Lyngby, Denmark*

(Dated: March 22, 2022)

We have carried out shear-deformation simulations on amorphous Mg-Cu systems at zero temperature and pressure, containing 2048-131072 atoms. At the largest size a smooth stress-strain curve is obtained with a well-defined flow stress. In the smallest system there are severe discontinuities in the stress-strain curve caused by localized plastic events. We show that the events can be characterized by a slip volume and a critical stress and we determine the distribution of these quantities from the ensemble of all events occurring in the small system. The distribution of critical stresses at which the enthalpy barriers for the individual events vanish is spread between 200 MPa and 500 MPa with a mean of 316 MPa, close to the flow stress observed in the largest system.

The mechanical properties of bulk metallic glasses[1, 2] (BMGs) are the subject of intense research. A host of applications is envisaged if only reasonable macroscopic plasticity could be achieved, rather than the intense localization into shear bands which typically occurs. Detailed knowledge of plastic deformation mechanisms in glasses, and their connection to macroscopic flow properties, however, remains elusive: While in crystals the dislocation provides a well defined starting point for estimates of flow stress, in glasses there is no such easily characterizable defect.

Various recent theories[3, 4] take as a starting point the existence of a collection of "relaxation centers"[3] or "shear-transformation zones"(STZs)[4, 5] which operate as localized centers of deformation. Based on a set of assumptions about the operation of the relaxation centers the total rate of plastic deformation is obtained from the collective behavior of the local centers.

Indeed, several simulations of deformation in amorphous metals[5, 6, 7, 8, 9] have established that the plastic behavior involves localized events with up to 150 atoms[6]. The transforming regions have been extensively studied from a potential energy landscape point of view by Lacks[8, 10, 11], and the response to shear and normal stresses have been investigated for Lennard-Jones systems[12]. In the latter work the connection between the properties of a single model STZ and the yield stress was discussed through the application of the Mohr-Coulomb yield criterion. Systematic studies of the dependence of macroscopic properties on the full ensemble of local deformation events, however, are still needed.

In this Letter, we describe zero temperature simulations of plastic deformation of a Cu-Mg glass and demonstrate a direct connection between the statistical properties of localized deformation events and the flow stress at mesoscopic length scales (10–100 nm). Our main results are (i) while for small systems the stress-strain curve shows sharp drops signifying individual deformation events, when the system size is over 10^5 atoms, the stress strain curve becomes quite smooth, with a clear flow stress of 320–330MPa (Fig.1); (ii) analysis of the individual events in the smallest system can be quantified in terms of two quantities, a critical stress σ_c and a quantity we call the "slip volume" V_{slip}; (iii) the mesoscopic flow stress is the mean of the distribution of σ_c, and the spatial density of transforming regions per unit strain in a large system is the inverse of the mean of V_{slip}.

The simulated material is $Mg_{0.85}Cu_{0.15}$, which is the optimal glass-forming composition for the Mg-Cu system[13]. This system is interesting because the addition of a small amount of Y makes it a BMG. The interatomic potential is the effective medium theory (EMT)[14], fitted to properties of the pure elements and intermetallic compounds obtained from experiment and density functional theory calculations. Details of the potential and of the method for creating the zero-temperature glassy configurations may be found in Ref. 15; for the 16384- and 131072-atom systems we have used the cooling rate of 0.72 K/ps. The main simulations involve continuous deformation of systems containing 2048, 16384 and 131072 atoms. The nominally zero-temperature configurations resulting from the cooling runs were further minimized before deformation runs, with respect to both atomic positions and the vectors describing the periodic supercell. The box vectors are in fact controlled by six strain degrees of freedom, which also play a role in the deformation simulations. We restrict to pure shear. The deformation simulations are strain-controlled: the relevant component of strain is incremented in steps of 0.0005. After each step the remaining degrees of freedom—the atomic positions and other strain components—are relaxed to minimize the energy.

Fig. 1 shows stress-strain curves for shear deformation simulations for three different system sizes. In all cases there is initially a smooth, almost linear increase, marking the elastic regime. In the smallest system, this is first interrupted by small kinks in the stress-strain curve, and then by sharp drops in stress. The remainder of the

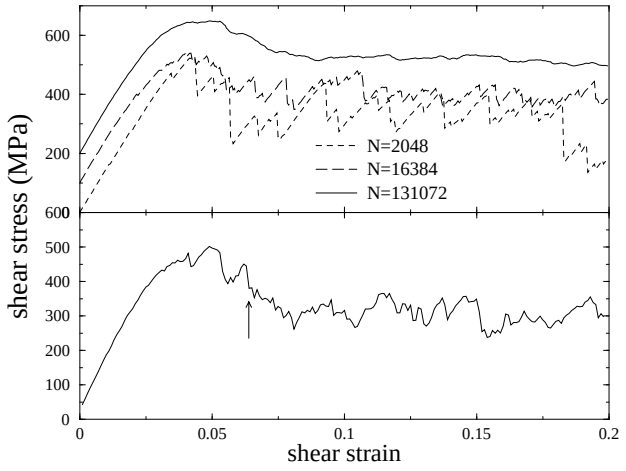


FIG. 1: Upper panel, stress-strain curves for different-sized systems undergoing pure shear at zero temperature, shifted for clarity. For the largest system the peak and flow stresses are 450MPa and 320MPa respectively, or about $\mu/16$ and $\mu/23$ where μ=7.3GPa is the shear modulus. Lower panel, stress-strain curve of a sub-volume of the 131072-atom system, selected because visualization (via deviation from affine

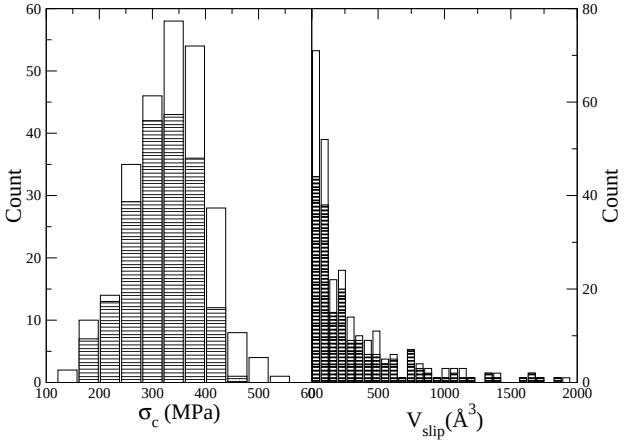


FIG. 2: Distribution of σ_c and $V_{\rm slip}$ values for all events (unshaded) and events taking place above 10% strain (shaded). The means are 331(316) MPa and 305(317) Å^3, where the figures in parentheses indicate the means of the shaded distributions.

curve is characterized by intervals of almost linear increase punctuated by further sharp drops. The highest stress attained is prior to the first significant drops. The size of fluctuations (drops) progressively diminishes for larger system sizes, so that for the 131072-atom system we observe a quite smooth curve with a well-defined flow stress following an initial peak.

A natural interpretation of the stress drops in the small system is that they represent discrete plastic flow "events", corresponding to the postulated STZs of theory or the localized events found in previous simulations. The fact that the slope of the stress curve between the drops is always the same indicates that here only elastic deformation is taking place and that the plastic deformation is entirely accounted for by processes associated with the drops. In the following we shall analyze the individual events, as identified in the small systems and use this information to address the properties of the large system. To confirm that the deformation of the large system also happens through localized events, we have used the technique from Ref. 5 to highlight atoms with a large deviation from affine deformation[21], and observing by direct visualization that the atoms so highlighted tend to form clusters, have generated statistics of these clusters. A cluster is a group of (at least three) so-highlighted atoms connected by nearest neighbor bonds. We count 5–7 clusters per nm^3 per unit strain in the "steady-state" regime between 10% and 20% strain. These clusters typically contain 3–20 atoms, although extreme cases involving up to 125 atoms also occur. In the small system an event marked by a stress drop typically involves one or two such clusters, thus we can use this system to study single events in detail.

The events are transitions involving internal rearrangements of atoms. We have identified two characteristic quantities associated with events. The first of these, termed "slip volume", is geometrical in nature and represents the amount of plastic strain associated with the event. The plastic strain is defined in terms of changes in the shape of the periodic simulation cell. However, if we take the event to be localized in the cell, the plastic strain induced at the boundaries depends not just on the geometry of the rearranging atoms but also on the volume of the cell. To see this, consider an idealized slip event as a planar area $A\hat{n}$ cut within the material, and the resulting free surfaces shifted relatively by an amount $\vec{b} \perp \hat{n}$, as in dislocation loop nucleation. Then the plastic shear strain felt by the boundary of the system is $\epsilon_{pl} \sim V_{\rm slip}/V$, where $V_{\rm slip} = bA$, and V is the system volume. Alternatively, knowing ϵ_{pl} we can multiply by V to obtain $V_{\rm slip}$. This slip volume is a tensorial quantity, but in this work we are only concerned with the component corresponding to the applied shear strain. We cannot decompose it into $\vec{b}$ and $A\hat{n}$, since the events are in general geometrically more complex than planar slip.

As we describe below we have determined the distribution of $V_{\rm slip}$, shown in the right panel of Fig. 2. Rather than being peaked at a finite value, the most likely value tends to zero. The distribution is in fact roughly exponential, although with some extra weight at large values: The mean is $\bar{V}_{\rm slip} \sim 305$Å^3; if an exponential is fitted to the initial data, a slightly smaller characteristic $V_{\rm slip}$ of 240 Å^3 is obtained. In a large system, the total strain can be written $\epsilon_{tot} = N_e \bar{V}_{\rm slip}/V$, where N_e is the total number of events. This implies that $\bar{V}_{\rm slip}^{-1} = 3.2{\rm nm}^{-3}$ is the number density of events per unit strain and volume. This is roughly a factor of two smaller than the num-

ber obtained by counting clusters; this is partly due to the fact that in the small system energetically isolated events may have more than one spatially separate cluster, and partly due to a possible enhancement of spatially separate events "cascading" together due to interactions with periodic images in a small system. Cascading has been studied by Maloney[16]. If we use the estimation of the mean from the exponential fit (which ignores excess large events) instead of the actual mean, we find an event density 4.2nm^{-3}, which is closer to that determined geometrically.

The second quantity is a *critical stress*, σ_c, the value of the shear stress at which the event happens spontaneously at T=0. At lower stresses, there exists a barrier which might be crossed due to thermal fluctuations at finite temperature, but at T=0 prevents the event from taking place until the stress rises high enough. To properly define σ_c we adopt a stress-controlled formalism, where the six strains all become degrees of freedom, and a stress term is added to the potential energy, with stress as a tunable parameter. There then exists a (3N+6)-dimensional potential energy (or enthalpy) landscape, which is effectively tilted by increasing the stress.

For each event apparent in the stress-strain curve, we take configurations from the simulation before and after the stress drop. These are close to minima of the enthalpy landscape. By minimization under a chosen stress we obtain locally stable configurations which we take as the "initial" and "final" states for the given event and the given stress. These are used to define V_{slip}. The enthalpy barrier between the events is determined using the Nudged Elastic Band method[17, 18, 19]. These are computed for a range of stresses sufficient to determine σ_c with accuracy; they are stress dependent, but the dependence is small in the case of V_{slip}, and was averaged over. We have taken pairs of configurations and calculated the above quantities in this way for every peak on the stress-strain curve from a shear deformation simulation of a 2048-atom system up to 30% strain.

Enthalpy profiles for a particular event are shown in Fig. 3. In the regime where the calculations have been done, i.e., fairly close to the critical stress at which the barrier vanishes (necessary for events to occur at T=0), the barrier is very small (1–10 meV) compared to the overall enthalpy change (∼1 eV). Also shown in the figure are the atoms most involved (determined by deviation from affine deformation). An animation of the process shows that the nature and order of the individual motions is as roughly indicated by the arrows. This event is relatively simple; some involve several tens of atoms and complex patterns of motion, although much of this can be decomposed into such small pieces involving snake-like motion and rotations of groups of three or four atoms.

The inset of Fig. 3 shows the barrier's stress dependence, whose form is a steady decrease with increasing stress, flattening out somewhat at the critical stress σ_c

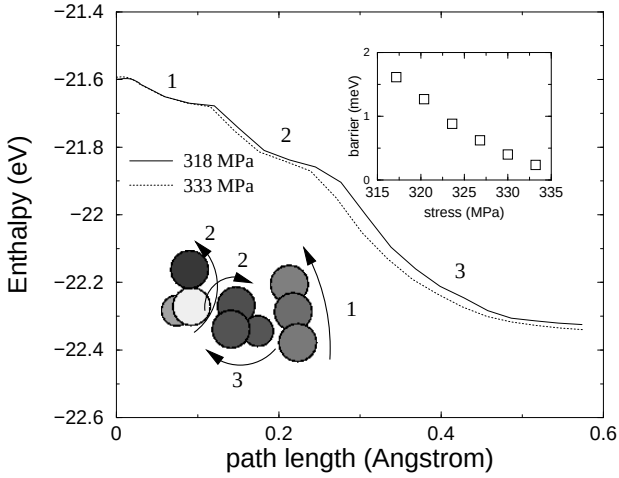


FIG. 3: Enthalpy along several minimum energy paths for an event, for different applied stresses as indicated; the barrier is just visible as a slight bump at the beginning of the path. In the bottom are shown the participating atoms, colored according to deviation from affine deformation computed between initial and final states, with arrows giving an indication of the types of motion and the numbers identifying the order of motions and the corresponding features in the enthalpy curve. Inset: stress-dependence of the barrier.

where the barrier vanishes. In fact, the barrier must vanish with a 3/2 power law sufficiently close to σ_c, due to the merging of a saddle-point and a local minimum of the enthalpy (as in a saddle-node bifurcation). The resolution of our data is not enough to identify this; simply using a linear or quadratic fit to the data near σ_c is sufficient to identify σ_c with an accuracy of ~ 2 MPa. The vanishing of the barrier (and the minimum) has been studied in detail by Malandro and Lacks[8, 10]. At lower stresses, there is extra structure in the barrier height, such as abrupt changes of slope or even local maxima.

In some cases an intermediate minimum was found along the minimum energy path, and in these cases separate calculations were made for each of the thus-identified "sub-events". By combining the results from all barrier determinations we can plot the distribution $g(\sigma_c)$ of critical stresses, shown in Fig. 2, left. To improve the statistics, we have also included events obtained by shear-deformation in the $x-z$ and $y-z$ planes, yielding a total of 262 events. There is a broad peak, with a mean of 331 MPa and a standard deviation of about 70 MPa. If we count only events taking place after 10% deformation (the shaded distribution in Fig. 2), the mean is a little lower, 316 MPa. This latter value is close to the flow stress observed in the large system.

Why is this? To obtain a connection between the deformation behavior of the small system and that of the large, we have computed the stress averaged over a subset of the 131072-atom system whose volume is that of the 2048-atom system. This stress-strain curve is plot-

ted in the lower part of Fig. 1. The striking feature of this curve is that it looks closer to that of the actual 2048-atom system than it does to that of the 131072-atom system as a whole, although the stress drops are not quite as large, nor as sharp. The particular subset was chosen to surround a cluster which was active at strain 0.064, and indeed a significant drop in the stress can be seen at that strain. The large system thus in a sense behaves as a collection of weakly coupled small systems, each undergoing relatively large stress fluctuations, but whose average is quite smooth. The fact that the stress drops are gentler than in the true 2048-atom system is presumably due the smaller constraints on this region provided by the surrounding material, compared to those of periodic boundary conditions; stress can relax into neighboring material during the relaxation to mechanical equilibrium.

Simple considerations provide crude estimates for the mesoscopic flow stress. In the manner of averaging elastic constants in polycrystals[20], we can assume that either the stress or the strain is uniform over subsystems. In the first case we imagine imposing a fixed stress on all subsystems and letting them respond independently. Then under relaxation, every subsystem will flow until it reaches the first critical stress that is higher than the imposed stress. No further deformation can take place—unless the imposed stress is higher than the maximum critical stress. Thus the flow stress is the maximum of the σ_c-distribution. This is at least an upper bound: The material clearly cannot sustain a stress greater than the maximum σ_c, 450 MPa for events taking place above 10% strain.

Alternatively, imposing a uniform strain on each subsystem, each undergoes deformation just like the single simulated small system. Assuming the individual stress-strain curves have no fixed phase relation, averaging across them at a given strain is equivalent to averaging over the strain history of a single subsystem. This average is straightforward to compute if the assumption of a fixed $V_{\rm slip}$ is made, yielding $\bar{\sigma}_c - \Delta\sigma/2$, where $\Delta\sigma = 2\mu V_{\rm slip}/V_{sub}$ is the stress drop associated with individual events in a subsystem. This value is 265 MPa with our choice of small system ($V_{sub} = 4.3 \times 10^4 \text{Å}^3$), about 10% less than the observed flow stress.

This estimate is necessarily rough, in particular because it explicitly involves an apparently arbitrary subsystem size. However, the size of our small system is not so arbitrary. We have previously noted that it corresponds more or less to the size at which events become discrete. Furthermore, analysis of the distribution of stress (not shown here) averaged over various-sized subsystems suggests that this size is about the smallest at which random fluctuations coming from the atomic stresses begin to cancel out enough to make the averaged stress meaningful—a quantity which actually represents force per unit area exerted by the material on itself. Apart from these considerations, the directly observed correspondence between the flow stress and the mean σ_c itself supports the overall picture of the statistics of small subsystems determining the mesoscopic plastic behavior.

This work was supported by the Danish Research Councils through Grant No. 5020-00-0012 and by the Danish Center for Scientific Computing through Grant No. HDW-1101-05.

* Electronic address: nbailey@fysik.dtu.dk

[1] A. L. Greer, Science **267**, 1947 (1995).
[2] W. L. Johnson, MRS Bulletin **24**, 42 (1999).
[3] V. A. Khonik, A. T. Kosilov, V. A. Mikhailov, and V. V. Sviridov, Acta. Mater. **46**, 3399 (1998).
[4] J. S. Langer, L. Pechenik, and M. L. Falk (2003), cond-mat/0311057.
[5] M. L. Falk and J. S. Langer, Phys. Rev. E **57**, 7192 (1998).
[6] D. Srolovitz, V. Vitek, and T. Egami, Acta. Metall. **31**, 335 (1982).
[7] K. Maeda and S. Takeuchi, Philos. Mag. A **44**, 643 (1981).
[8] D. L. Malandro and D. J. Lacks, J. Chem. Phys. **110**, 4593 (1999).
[9] A. C. Lund and C. A. Schuh, Acta Mater. **51**, 5399 (2003).
[10] D. L. Malandro and D. J. Lacks, Phys. Rev. Lett. **81**, 5576 (1998).
[11] D. J. Lacks, Phys. Rev. Lett. **87**, 225502 (2001).
[12] A. C. Lund and C. A. Schuh, Nature Mater. **2**, 449 (2003).
[13] F. Sommer, G. Bucher, and B. Predal, J. Phys. Colloque C8 **41**, 563 (1980).
[14] K. W. Jacobsen, P. Stoltze, and J. K. Nørskov, Surf. Sci. **366**, 394 (1996).
[15] N. P. Bailey, J. Schiøtz, and K. W. Jacobsen, Phys. Rev. B **69**, 144205 (2004).
[16] C. Maloney and A. LeMaître (2004), cond-mat/0402148.
[17] H. Jónsson, G. Mills, and K. W. Jacobsen, in *Classical and Quantum Dynamics in Condensed Phase Simulations*, edited by B. J. Berne, G. Ciccotti, and D. F. Coker (World Scientific, 1998).
[18] G. Henkelman and H. Jónsson, J. Chem. Phys. **113**, 9978 (2000).
[19] G. Henkelman, B. Uberuaga, and H. Jónsson, J. Chem. Phys. **113**, 9901 (2000).
[20] J. P. Hirth and J. Lothe, *Theory of Dislocations* (Krieger Publishing Company, 1982), 2nd ed.
[21] We compare configurations differing in strain by 0.1% and use a cutoff of 10 Å^2, consistent with that used in Ref. 5.